Supporting Information

Ultrafast Exciton–Polaron Dynamics in Moiré Superlattices

Junais Habeeb Mokkath

junais.mokkath@aasu.edu.kw

College of Integrative Studies, Abdullah Al Salem University (AASU), Block 3, Khaldiya, Kuwait.

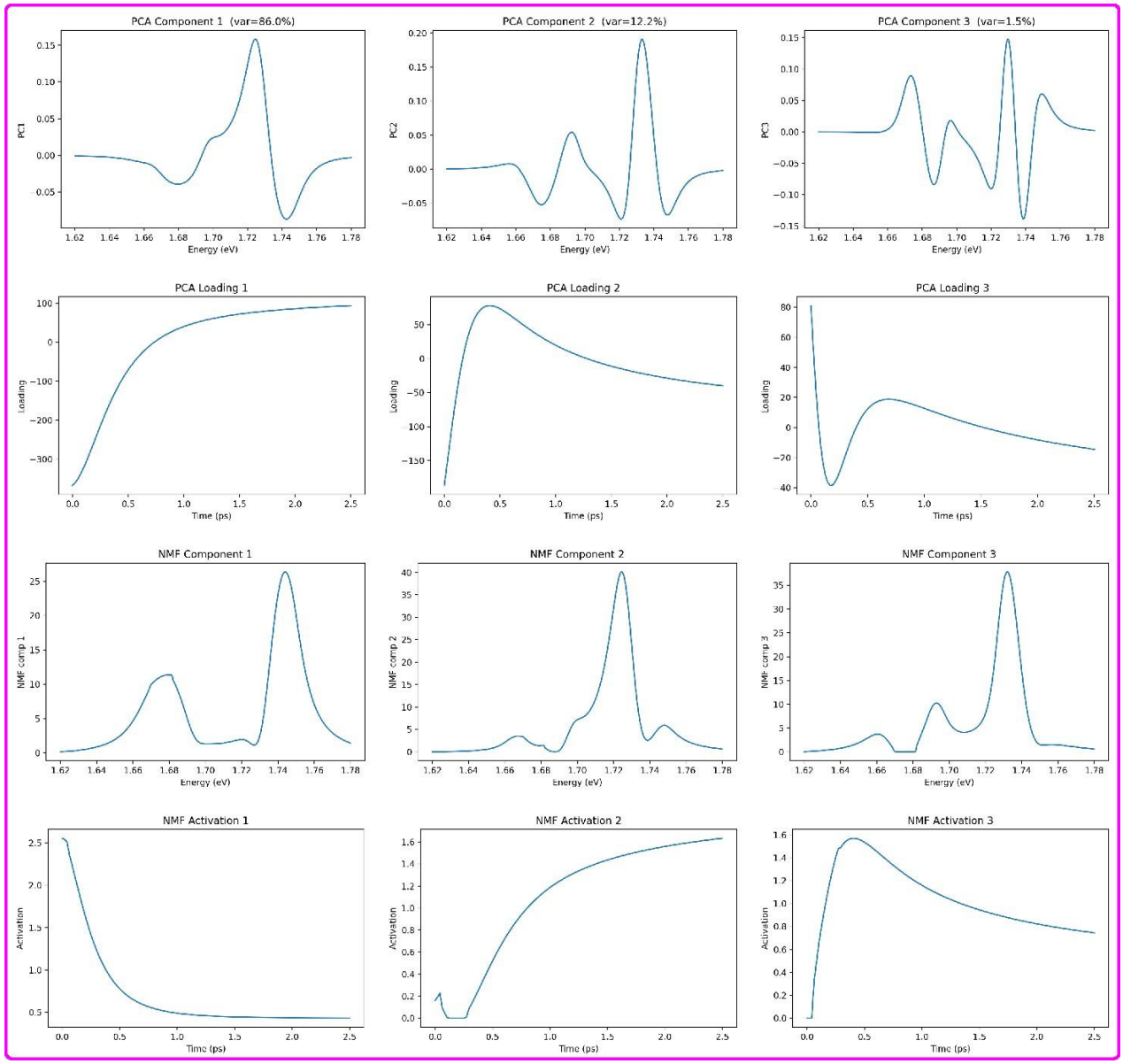

Figure S1: Principal Component and Non-negative Matrix Factorization (NMF) decomposition of transient spectra. The top two rows show the results of principal component analysis (PCA), where the first three spectral components (top row) and their corresponding temporal loadings (second row) capture 86%, 12%, and 1.5% of the total variance, respectively. These components represent dominant spectral–temporal correlations associated with the lower and upper polariton branches and their evolution after excitation. The bottom two rows present the NMF decomposition, separating the transient signal into three physically interpretable components with distinct spectral features (bottom-left panels) and corresponding time-dependent activations (bottom-right panels). NMF component 1 corresponds to the exciton bleach, component 2 captures the induced absorption of the exciton–polaron branch, and component 3 represents higher-energy polariton dynamics. Together, these analyses reveal the minimal basis set describing the ultrafast exciton–polaron–polariton evolution.

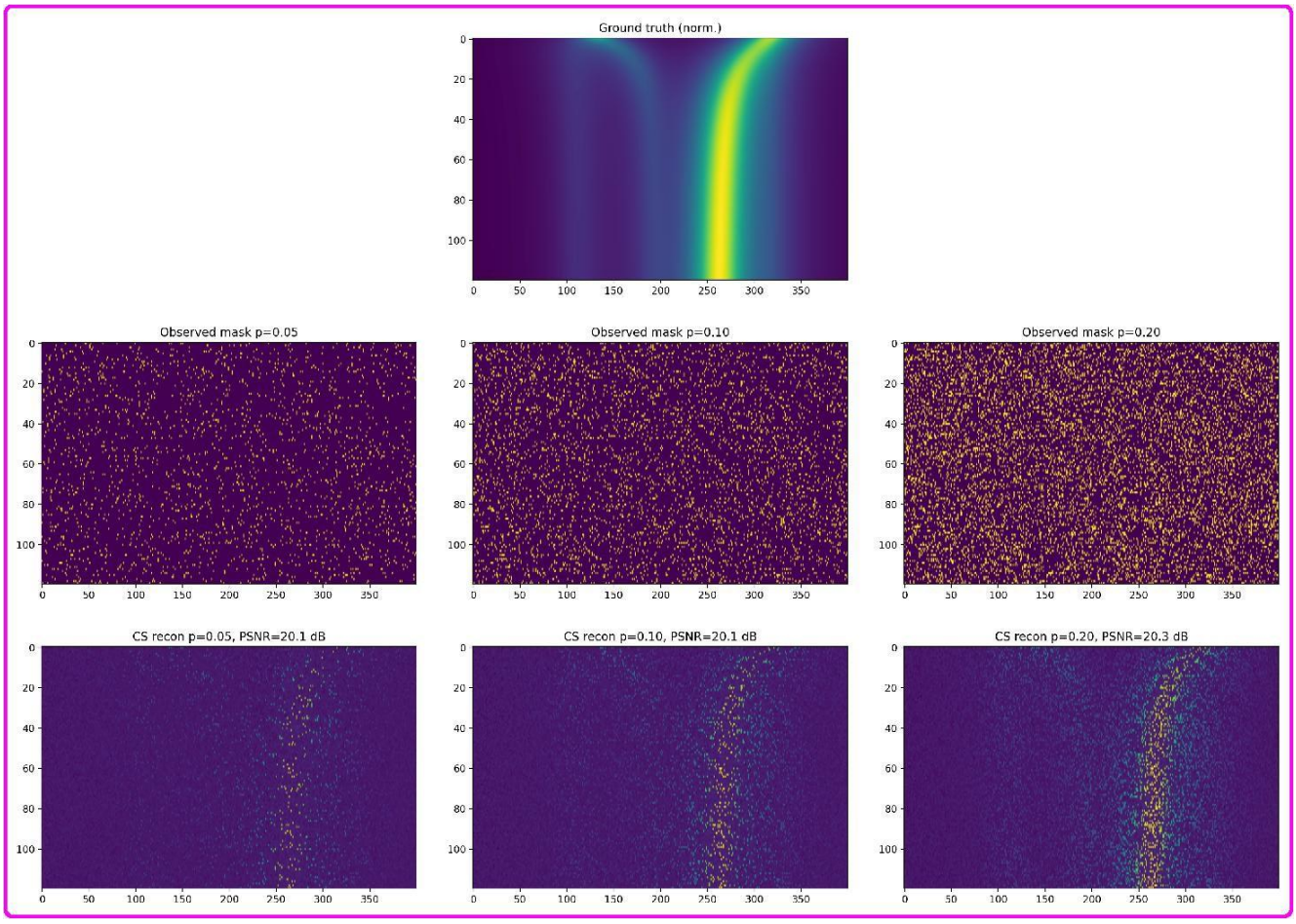

Figure S2: Compressed sensing reconstruction of transient spectral dynamics under sparse sampling. The top panel shows the normalized ground-truth transient spectrum used as a reference. The middle row presents randomly sampled observation masks with increasing sampling density ($p = 0.05$, 0.10, and 0.20), corresponding to 5–20% of the total data points acquired. The bottom row shows the reconstructed spectra obtained via compressed sensing (CS) using an ℓ_1-regularized solver. Even at low sampling ratios, the recovered data preserves the key spectral–temporal features of the original map with minimal distortion, achieving PSNR values of approximately 20 dB across all cases. This demonstrates that CS-based acquisition can substantially reduce measurement time while maintaining quantitative fidelity in ultrafast nanoscale imaging.

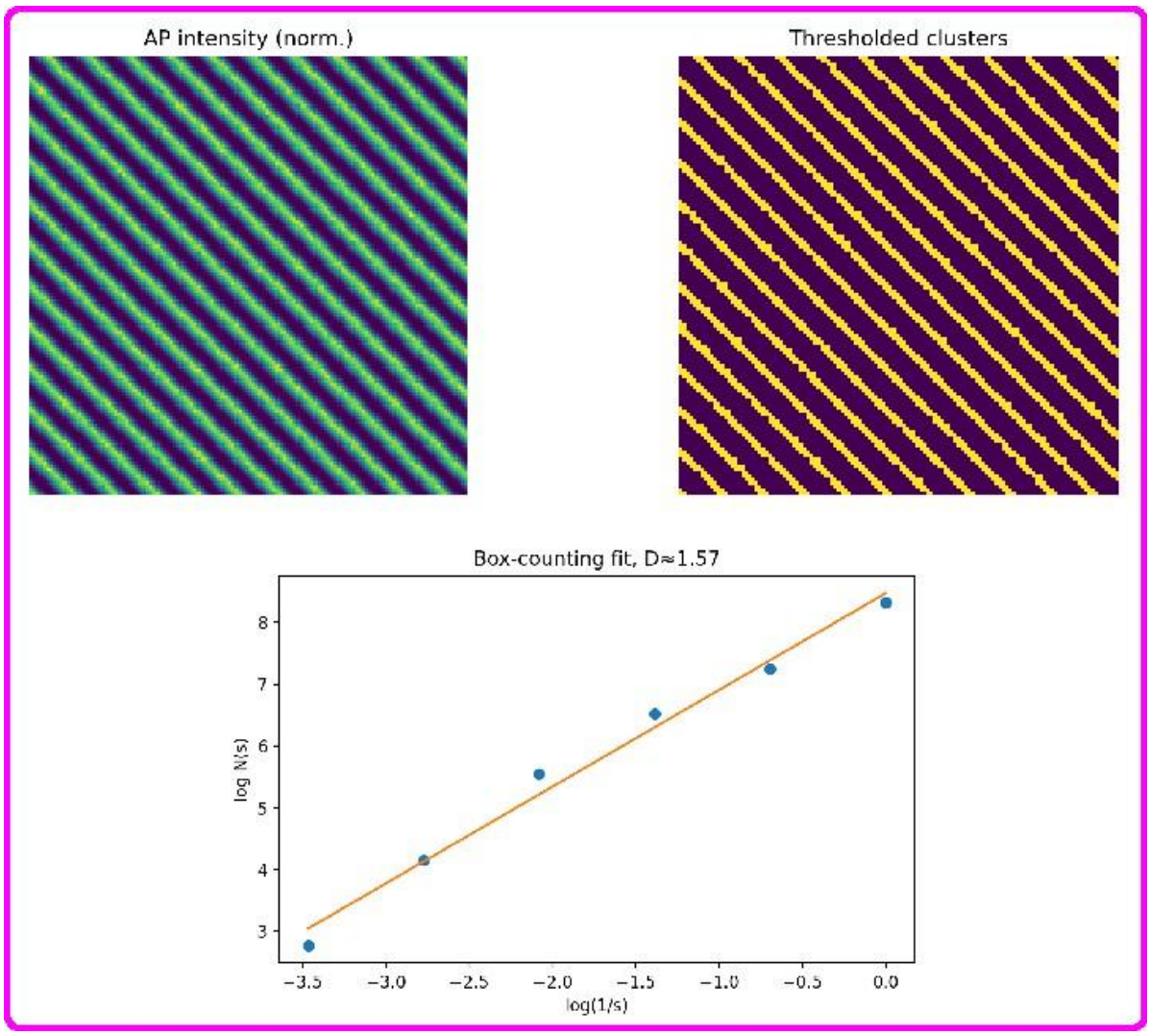

Figure S3: Fractal analysis of spatially modulated absorption pattern. The top panels show the normalized absorption–polariton (AP) intensity map and its corresponding thresholded binary cluster representation. The self-similar periodic domain structure exhibits clear spatial correlations indicative of hierarchical pattern formation. The bottom panel presents the box-counting analysis used to estimate the fractal dimension ($D \approx 1.57$), confirming an intermediate scaling regime between one- and two-dimensional order. This suggests the presence of correlated nanoscale domains that emerge from exciton–polariton field interference and spatial coupling.

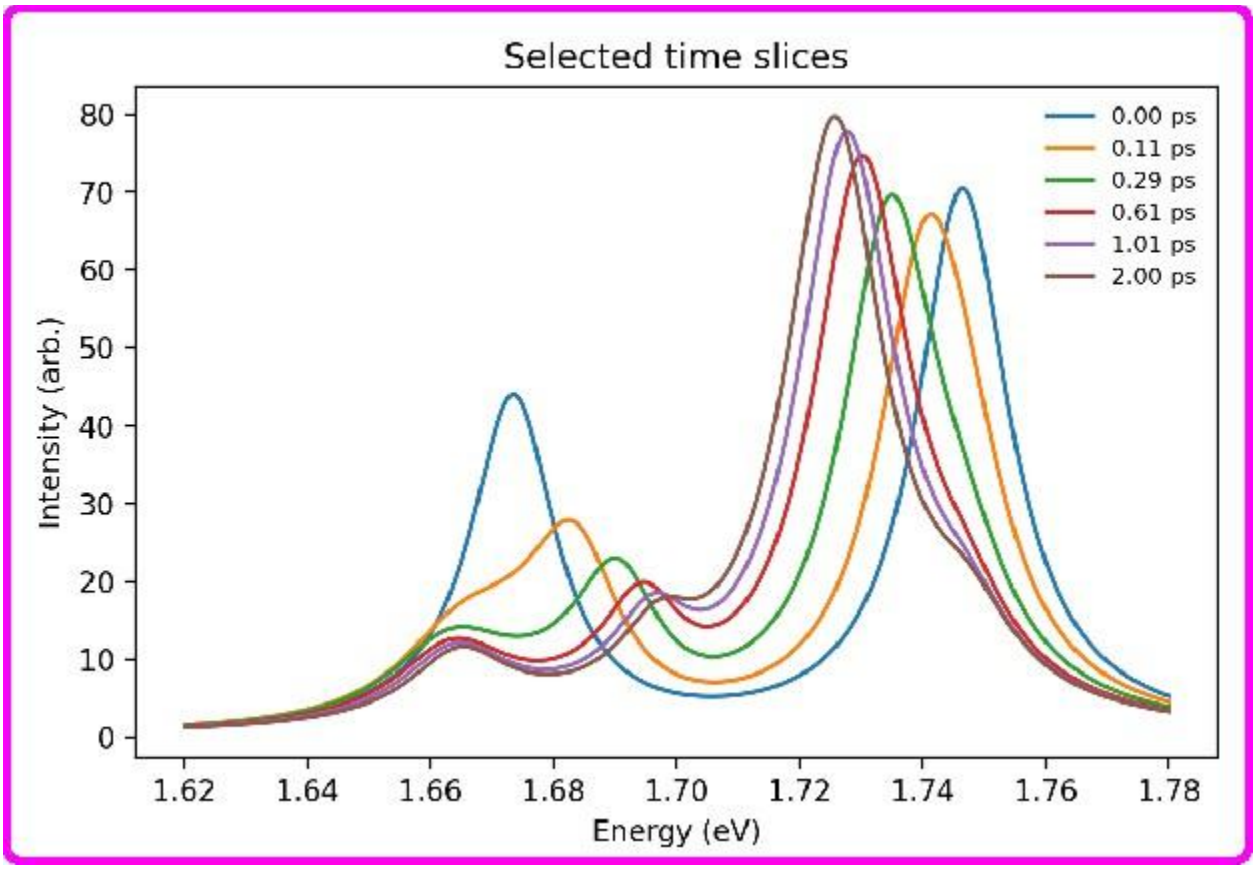

Figure S4: Time-resolved spectral evolution of exciton–polariton branches. Transient spectra at selected time delays reveal the temporal evolution of the lower (LP), upper (UP), and exciton–polaron (AP) resonances following optical excitation. The initial splitting near $t = 0$ indicates strong light–matter coupling, while subsequent spectral shifts and intensity redistribution reflect relaxation and dephasing processes within the moiré superlattice. The progressive narrowing and redshift of the UP feature correspond to energy dissipation and exciton–polaron dressing over picosecond timescales.

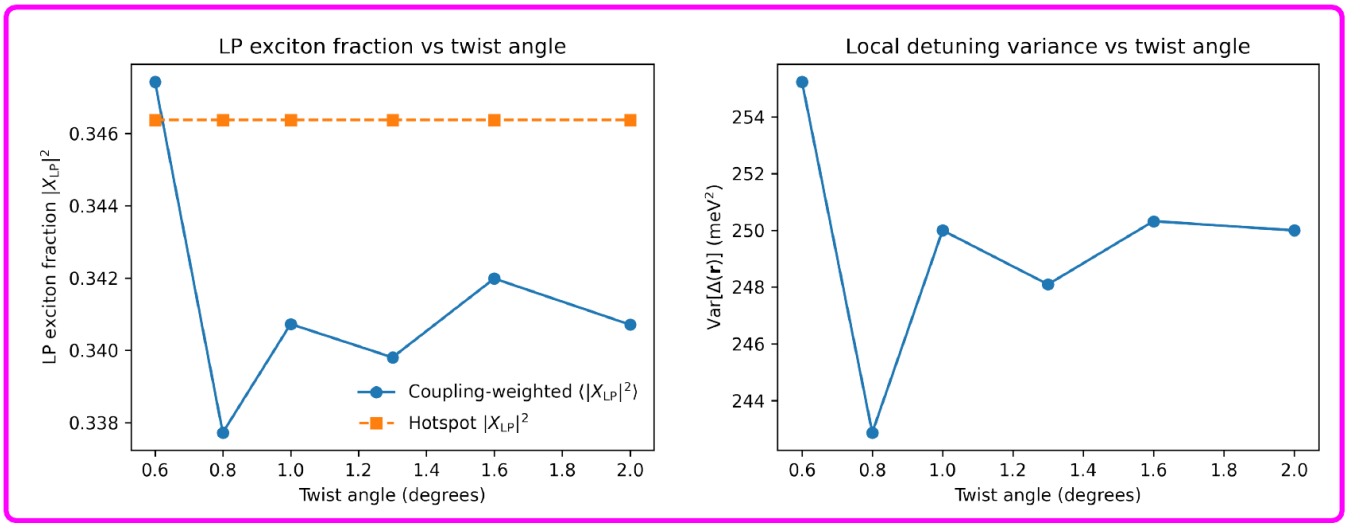

Figure S5: Twist-angle dependence of lower-polariton properties. Left: Lower-polariton exciton fraction $|X_{\mathrm{LP}}|^2$ as a function of twist angle, comparing coupling-weighted spatial averages and hotspot values. Right: Variance of the local exciton--cavity detuning induced by the moiré potential versus twist angle, reflecting enhanced spatial modulation at smaller moiré periods

Photoexcitation protocol

Photoexcitation is modeled as a time-dependent driving term acting on the excitonic transition, representing an impulsive optical pump. The excitation enters the Hamiltonian as

$$H_{\mathrm{drive}}(t) = \Omega(t)(|X\rangle\langle 0| + |0\rangle\langle X|)$$

where $\Omega(t)$ denotes the temporal envelope of the pump pulse. In this work, $\Omega(t)$ is chosen as a short Gaussian pulse, creating an initial excitonic coherence and population that subsequently evolve under non-Hermitian exciton--polariton dynamics. This minimal description captures the essential physics of ultrafast photoexcitation while avoiding explicit treatment of the optical field.

Transient spectrum and spectral map

The transient optical spectrum is calculated from the time-dependent excitonic polarization $P(t) = \langle 0|\rho(t)|X\rangle$ obtained from the non-Hermitian quantum dynamics. The frequency-resolved response is computed using a short-time Fourier transform,

$$S(\omega, t) = \left| \int_{t}^{t+T_w} P(t')\, e^{i\omega t'}\, dt' \right|^2$$

where T_w denotes the temporal window over which the transform is evaluated. A Lorentzian broadening consistent with the excitonic and photonic linewidths is applied to account for finite spectral resolution. The spectral map is defined as the intensity $S(\omega, t)$ plotted as a function of frequency ω and time delay t, providing a direct visualization of the temporal evolution of polaritonic resonances. This representation allows tracking of peak positions, linewidths, and spectral weight transfer during exciton--polaron--polariton formation.

Local coupling strength and detuning

Spatial variations of the exciton--photon interaction arise from the combined effects of the moiré-localized exciton wavefunction and the cavity field profile. The local coupling strength is defined as

$$g(\mathbf{r}) = \frac{\mu}{\hbar} E_0(\mathbf{r}) \, |\psi_X(\mathbf{r})|$$

where μ is the excitonic transition dipole moment, $E_0(\mathbf{r})$ denotes the spatial profile of the cavity electric field, and $\psi_X(\mathbf{r})$ is the exciton wavefunction localized by the moiré potential. This definition captures the enhancement or suppression of light--matter coupling at different moiré sites. The local detuning is defined as

$$\Delta(\mathbf{r}) = E_C - [E_X + V(\mathbf{r})],$$

where E_C is the cavity resonance energy, E_X is the bare exciton energy, and $V(\mathbf{r})$ is the moiré potential. As a result, spatial modulation of the exciton energy directly translates into a site-dependent detuning landscape. This framework enables systematic exploration of detuning-coupling maps and local polaritonic dynamics without introducing additional material-specific fitting parameters.

Electrostatic gating and charge density

Electrostatic gating and finite charge density are incorporated in the model at a phenomenological level. Rather than solving a self-consistent electrostatic problem, the effect of carrier doping is captured through renormalized excitonic parameters, including shifts in the exciton energy, modifications of the effective linewidth, and redistribution of spectral weight among neutral exciton and polaronic states. These effects are motivated by experimentally observed gating-induced exciton--polaron formation in charge-tunable TMD systems. The resulting density dependence enters the non-Hermitian dynamics through effective energies and decay rates, allowing systematic exploration of gating trends without introducing additional microscopic complexity.